Available online at www.sciencedirect.com

ScienceDirect

Mendeleev Commun., 2023, **33**, 422–424

Mendeleev Communications

Formation of active phases of Fe/C, Cr/C and Fe–Cr/C catalysts in oxidative dehydrogenation of ethane

Igor I. Mishanin,*[a,b] Tatiana V. Bogdan,[a,b] Aleksey V. Smirnov,[a,b] Petr A. Chernavskii,[a,b] Natalia N. Kuznetsova[b] and Viktor I. Bogdan*[a]

[a] *N. D. Zelinsky Institute of Organic Chemistry, Russian Academy of Sciences, 119991 Moscow, Russian Federation. E-mail: mishanin@ioc.ac.ru, vibogdan@gmail.com*

[b] *Department of Chemistry, M. V. Lomonosov Moscow State University, 119991 Moscow, Russian Federation*

DOI: 10.1016/j.mencom.2023.04.039

The oxidative dehydrogenation of ethane into ethylene using CO_2 as an oxidant at temperatures of 650–750 °C was carried out over Fe/C, Cr/C and Fe–Cr/C catalysts deposited on a carbon support. Before and after the reaction the catalysts were investigated by X-ray powder diffraction (XRD), *in situ* magnetometry and transmission electron microscopy methods. The correlation between activity of Fe/C, Cr/C and Fe–Cr/C catalytic systems and their phase composition was established.

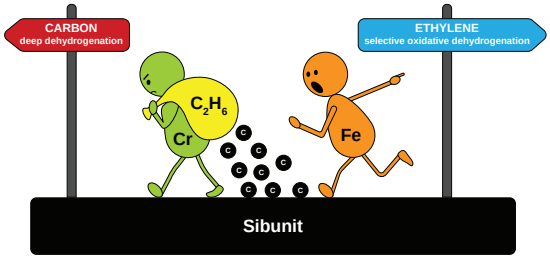

Keywords: oxidative dehydrogenation of ethane into ethylene, carbon dioxide, Fe/C catalyst, Cr/C catalyst, Fe–Cr/C catalyst, XRD, magnetometry, TEM.

Light olefins, in particular ethylene and propylene, are the most important raw materials in petrochemical industry.[1–4] Over the past decades researchers have come much closer to the industrial implementation[5] of ethylene production *via* oxidative dehydrogenation (ODH) of ethane. The ethane ODH process is usually investigated at atmospheric pressure, although there are a number of studies where a positive effect of increasing the total reaction pressure on selectivity and performance for the target olefin has been noted.[6–8] Oxygen[9,10] and carbon dioxide[11–14] are most commonly employed oxidizing agents. Using CO_2 as an oxidant allows one not only to work safely with hydrocarbon mixtures and increase the ethylene yield compared with the direct dehydrogenation, but also to solve the problem of carbon dioxide utilization. It is promising to conduct ODH using heterogeneous catalysts, among which Cr and Fe based catalysts are the most suitable for production needs since iron and chromium oxides are available substances that have proven their catalytic efficiency in the ethane ODH process.[15] In heterogeneous catalysis, both the chemical nature of the catalyst and the support for the active substance play an important role. It has been revealed that *in situ* regeneration of the catalyst in the CO_2 flow[16] is possible owing to the reducing properties of carbon substrate.

Herein, we focused on the establishing the correlation between phase composition of Fe/C, Cr/C and Fe–Cr/C catalysts and their activity in the ODH of ethane. The aim of the work was also to compare the phase composition of Fe/C, Cr/C and Fe–Cr/C catalysts by *in situ* magnetometry, X-ray powder diffraction (XRD) and transmission electron microscopy (TEM) methods and to explore the transformations taking place in the catalysts during the ODH process.

Samples of catalysts were prepared by impregnation according to moisture capacity from nitrates of the corresponding salts.[†] The mass content of metal in the catalysts was 5 wt% Fe in Fe/C, 5 wt% Cr in Cr/C, 5 wt% Fe and 5 wt% Cr in Fe–Cr/C. The ODH process was carried out in a quartz flow-type reactor at atmospheric pressure in the temperature range of 650–750 °C. The catalyst loading was 1 g, the feed rates of reagents $v(C_2H_6) = v(CO_2) = 25$ ml min^{-1}. The values of activity and selectivity were measured after 60 min of ethane ODH at a given temperature. The phase composition analysis of the catalysts was carried out by *in situ* magnetometry,[17] X-ray phase analysis and TEM.[†] The reaction products were analyzed by gas chromatography on LHM-80 chromatographs with thermal conductivity detectors using two printed columns: Porapak Q for hydrocarbons analysis, CO and CO_2 (He carrier gas) and CaA (5Å) for H_2 analysis (Ar carrier gas).

During the ODH of ethane with CO_2, C_2H_4, CO, H_2, H_2O, CH_4 and C are formed according to reactions:

$$C_2H_6 \rightarrow C_2H_4 + H_2 \qquad \Delta G^0 = 140.93 - 0.131T \text{ (kJ mol}^{-1}\text{)}, \quad (1)$$

$$C_2H_4 \rightarrow C_2H_2 + H_2 \qquad \Delta G^0 = 181.12 - 0.129T \text{ (kJ mol}^{-1}\text{)}, \quad (2)$$

$$C_2H_2 \rightarrow 2C + H_2 \qquad \Delta G^0 = -226.43 + 0.056T \text{ (kJ mol}^{-1}\text{)}, \quad (3)$$

$$C + 2H_2 \rightarrow CH_4 \qquad \Delta G^0 = -81.829 + 0.1003T \text{ (kJ mol}^{-1}\text{)}, \quad (4)$$

$$CO_2 + H_2 \rightarrow CO + H_2O \qquad \Delta G^0 = 38.261 - 0.0356T \text{ (kJ mol}^{-1}\text{)}, \quad (5)$$

$$CO_2 + C \rightarrow 2\,CO \qquad \Delta G^0 = 172.82 - 0.1776T \text{ (kJ mol}^{-1}\text{)}. \quad (6)$$

The results of catalytic experiments indicating the mass ratio of products are shown in Table 1. For all catalysts ethylene productivity increased significantly with the temperature rise. The proportion of carbon in the products has also grown markedly with the temperature, as at 750 °C the processes of

[†] See details in Online Supplementary Materials.

Table 1 Results of oxidative dehydrogenation of ethane into ethylene using CO_2 as an oxidant over Fe/C, Cr/C and Fe–Cr/C catalysts.

Catalyst	*T*/°C	X reagent activity/ $g_X\ g_{cat}^{-1}\ h^{-1}$		Product mass content (%)					
		C_2H_6	CO_2	CO	CH_4	C_2H_4	H_2	H_2O^a	C^b
Fe/C	650	0.15	0.21	61	2	15	1	21	0
	700	0.32	0.62	58	2	16	2	19	3
	750	0.74	1.09	48	2	19	2	23	6
Cr/C	650	0.59	0.92	63	6	19	3	7	2
	700	0.84	1.33	51	5	13	2	19	10
	750	0.85	1.42	39	3	16	2	24	16
Fe–Cr/C	650	0.30	0.55	64	5	22	1	8	0
	700	0.58	1.06	58	5	19	1	15	2
	750	0.84	1.27	42	4	24	1	23	6

[a] The amount of water formed was estimated as: $n(H_2O) = 2n(CO_2)_0 - 2n(CO_2) - n(CO)$, where $n(CO_2)_0$ is an initial amount of CO_2 and $n(CO_2)$ after the reaction. [b] The amount of carbon was estimated as: $n(C) = 2n(C_2H_6)_0 + n(CO_2)_0 - 2n(C_2H_6) - n(CO_2) - 2n(C_2H_4) - n(CH_4) - n(CO)$.

deep dehydrogenation of ethane with methane and carbon formation become more thermodynamically advantageous. The mass fraction of water in the products over the entire temperature range accounts for about 20% at 700–750 °C; and for the Fe/C catalyst it is also observed at 650 °C due to the active water gas reaction [equation (5)]. The diagram (Figure 1) presents our data on the performance of the basic ethane ODH products over Fe/C, Cr/C and Fe–Cr/C catalysts at 700 °C.

As is known, chromium-based catalysts are strong dehydrogenation agents and the highest ethane conversion occurs at Cr/C. However, the reaction proceeds non-selectively: due to ethane deep dehydrogenation methane is produced and a strong surface coking takes place. The intermediate activity value for the Fe–Cr/C catalyst indicates the formation of less active compounds. The combination of two metal components in the Fe–Cr/C catalyst results in the significant increase in ethylene yield relative to Fe/C and in the decrease in surface carbonization. An important factor reducing the carbonization of catalysts (see Figure S1, Online Supplementary Materials) is an occurring Boudouard–Bell reaction [equation (6)].

To explain the obtained regularities, a physicochemical study of the structure and phase composition of the catalysts before and after the reaction was carried out. Fe-containing catalysts were studied by magnetometry. The magnetization curves of the catalysts are shown in Figure 2. The presence of the Fe_3O_4 magnetite phase was revealed in the Fe/C sample before the reaction. After the reaction, the magnetization of the Fe/C sample increases by 6.5 times, in this case the magnetization *vs.* temperature dependence is very complicated (see curve *2*, Figure 2). Determination of the Curie temperature makes it

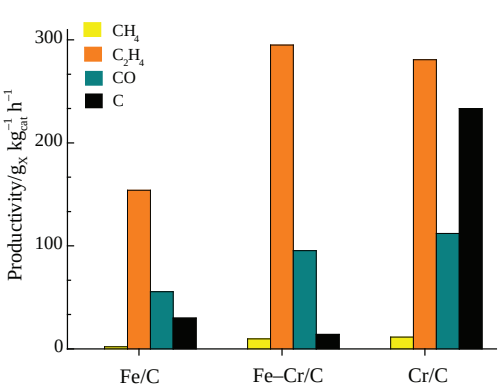

Figure 1 Productivity to the main products in the ODH process at 700 °C.

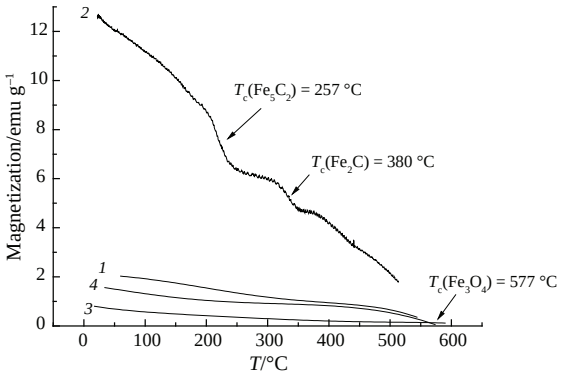

Figure 2 Temperature dependence of magnetization for Fe/C catalysts: (*1*) before ODH and (*2*) after ODH; and for Fe–Cr/C: (*3*) before ODH and (*4*) after ODH.

possible to identify the phases of magnetite Fe_3O_4 and iron carbides Fe_5C_2 and Fe_2C. Therefore, during ODH the phase composition of the Fe/C catalyst and its magnetic properties change significantly.

The magnetization of the Fe–Cr/C catalyst is significantly lower in comparison with the Fe/C sample. It is safe to suggest that in this sample the magnetite phase is occurred in a small amount. A slight increase in magnetization after the reaction is probably due to the reduction of iron in the catalyst to a metallic state in the presence of carbon support.

XRD data for the catalysts before and after the reaction are shown in Figure 3. The Fe_3O_4 magnetite phase was identified for the Fe/C catalyst before the reaction. After the reaction the intensity of magnetite reflexes reduces and new reflexes appear at 36 and 42° that correspond to metallic iron and/or its carbides. Thus, an increase in the magnetization of the Fe/C catalyst after the reaction is due to the formation of iron and/or its carbides.

The reflexes positions on the diffractograms of the Fe–Cr/C catalyst before and after the reaction are the same, they also coincide with the reflexes on the Fe/C diffractogram before the reaction, where the magnetite phase was detected. However, according to the magnetometry data (see Figure 2), the magnetite phase is contained in the Fe–Cr/C catalyst in a smaller amount than in Fe/C, *i.e.* a non-magnetic phase with lattice parameters close to magnetite was formed on the surface of the Fe–Cr/C catalyst. The lattice parameters of magnetite Fe_3O_4 and iron chromite $FeCr_2O_4$ are almost identical, that gives grounds to consider the non-magnetic phase of iron chromite as the main component of the Fe–Cr/C catalyst. The distinction in the Fe–Cr/C diffractograms before and after the ODH is marked by the increase in the height of reflexes, which indicates the improvement of catalyst crystallinity during the reaction. In addition, the new reflex at $2\theta = 50°$ emerges on the diffractogram of sample after ODH. Given that the magnetization of Fe–Cr/C

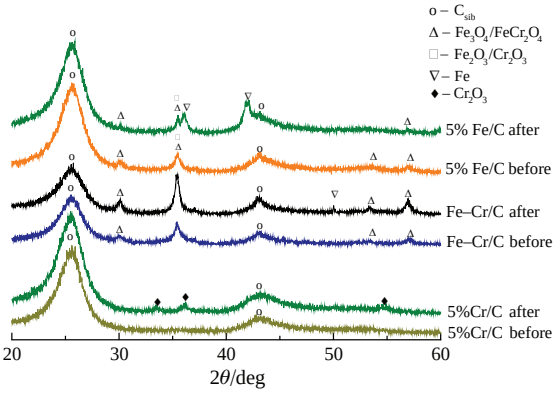

Figure 3 XRD patterns of Fe/C, Cr/C and Fe–Cr/C catalysts before and after ODH.

goes up after the reaction, the appearance of this reflex relates to the magnetic phases of metallic iron and its carbides.

The broad maxima on the diffractogram of the Cr/C catalyst before the reaction correspond to the carbon support. Thus, chromium on the support surface occurs in a highly dispersed state. After the reaction reflexes at 2θ of 33–36 and 55° appear which correspond to the Cr_2O_3 phase. The surface of the Cr/C catalyst has been studied by TEM. Micrographs of the catalyst prior to reaction are given in Figure S2. X-ray analysis revealed the finely dispersed state of the metal. The distribution of the elements over the catalyst surface determined *via* energy-dispersive X-ray spectroscopy (see Figure S3) shows that chromium is predominantly in the form of oxides. After the reaction the crystallite formation on the surface of the catalyst has been revealed; these crystallites exhibit a clear diffraction pattern which allows one to determine the phase composition. The following phases have been identified: metal chromium, chromium carbide Cr_3C_2 and oxides Cr_2O_3 and CrO_3 (see Figure S4). Therefore, the Cr/C specimen is a polyphase system subject to reduction/oxidation processes under activation and in the ODH process.

Thus, the phase composition of catalysts changes under the ethane ODH conditions, which is most expressed for Cr/C and Fe/C monometallic compositions. The Fe/C catalyst containing Fe_3O_4 magnetite as the basic surface phase shows the lowest activity in the ethane ODH. After the reaction the magnetization of the sample increases significantly; the phases of magnetite Fe_3O_4 and iron carbides Fe_5C_2 and Fe_2C have been identified. The Cr/C catalyst is a polyphase system subject to reduction/oxidation processes in the reaction of the ethane ODH. This causes the highest total conversion of ethane with extremely non-selective complete dehydrogenation of ethane into carbon. The combination of iron and chromium in the Fe–Cr/C catalyst results in the decrease in carbon yield, as compared with that for Cr/C, whereas the ethylene yield is high and selective. The iron chromite $FeCr_2O_4$ phase, active and highly selective in oxidative dehydrogenation of ethane into ethylene, was revealed in the two-component Fe–Cr/C catalyst before and after the reaction. Other carbide and oxide phases characteristic of monometallic samples have been present in minor amounts.

The research was supported by the Russian Science Foundation (grant no. 22-73-00119, https://rscf.ru/project/22-73-00119/). The authors are grateful to S. V. Savilov and S. V. Maksimov (Department of Chemistry of Moscow State University) for conducting research using the TEM method at the Moscow State University Centre for Collective Use ‘Nanochemistry and Nanomaterials’ within the framework of the MSU Development Program. The authors also express gratitude to Dr. Sci. I. V. Mishin (Institute of Organic Chemistry of the Russian Academy of Sciences) for the study of samples by XRD.

Online Supplementary Materials

Supplementary data associated with this article can be found in the online version at doi: 10.1016/j.mencom.2023.04.039.

References

1 T. Ren, M. Patel and K. Blok, *Energy*, 2006, **31**, 425.
2 M. A. Tedeeva, A. L. Kustov, P. V. Pribytkov, G. I. Kapustin, A. V. Leonov, O. P. Tkachenko, O. B. Tursunov, N. D. Evdokimenko and L. M. Kustov, *Fuel*, 2022, **313**, 122698.
3 S. Wang, K. Murata, T. Hayakawa and K. Suzuki, *Appl. Catal., A*, 2000, **196**, 1.
4 S. A. Chernyak, M. Corda, J. P. Dath, V. V. Ordomsky and A.Y. Khodakov, *Chem. Soc. Rev.*, 2022, **51**, 7994.
5 X. Wang, Y. Wang, B. Robinson, Q. Wang and J. Hu, *J. Catal.*, 2022, **413**, 138.
6 I. I. Mishanin and V. I. Bogdan, *Mendeleev Commun.*, 2019, **29**, 455.
7 J. Chen, Z. Sun, V. Balakotaiah and P. Bollini, *Chem. Eng. J.*, 2022, **445**, 136605.
8 E. S. Alekseev, A. Yu. Alentiev, A. S. Belova, V. I. Bogdan, T. V. Bogdan, A. V. Bystrova, E. R. Gafarova, E. N. Golubeva, E. A. Grebenik, O. I. Gromov, V. A. Davankov, S. G. Zlotin, M. G. Kiselev, A. E. Koklin, Yu. N. Kononevich, A. E. Lazhko, V. V. Lunin, S. E. Lyubimov, O. N. Martyanov, I. I. Mishanin, A. M. Muzafarov, N. S. Nesterov, A. Yu. Nikolaev, R. D. Oparin, O. O. Parenago, O. P. Parenago, Y. A. Pokusaeva, I. A. Ronova, A. B. Solovieva, M. N. Temnikov, P. S. Timashev, O. V. Turova, E. V. Filatova, A. A. Philippov, A. M. Chibiryaev and A. S. Shalygin, *Russ. Chem. Rev.*, 2020, **89**, 1337.
9 D. A. Svintsitskiy, T. Yu. Kardash, E. V. Lazareva, A. A. Saraev, E. A. Derevyannikova, M. Vorokhta, B. Šmíd and V. M. Bondareva, *Appl. Catal., A*, 2019, **579**, 141.
10 S. Rostom and H. de Lasa, *Catalysts*, 2020, **10**, 418.
11 T.-q. Lei, Y.-h. Cheng, C.-x. Miao, W.-m. Hua, Y.-h. Yue and Z. Gao, *Fuel Process. Technol.*, 2018, **177**, 246.
12 A. Bakhtyari, S. Zafarnak, H. Taghvaei, M. R. Rahimpour and A. Iulianelli, *J. CO2 Util.*, 2021, **47**, 101499.
13 T. A. Bugrova, V. V. Dutov, V. A. Svetlichnyi, V. C. Corberán and G. V. Mamontov, *Catal. Today*, 2019, **333**, 71.
14 Y. Abdelbaki, A. de Arriba, B. Solsona, D. Delgado, E. García-González, R. Issaadi and J. M. López Nieto, *Appl. Catal., A*, 2021, **623**, 118242.
15 I. I. Mishanin, T. V. Bogdan, A. E. Koklin and V. I. Bogdan, *Chem. Eng. J.*, 2022, **446**, 137184.
16 I. I. Mishanin and V. I. Bogdan, *Mendeleev Commun.*, 2020, **30**, 359.
17 P. A. Chernavskii, G. V. Pankina and V. V. Lunin, *Russ. Chem. Rev.*, 2011, **80**, 579.

Received: 18th October 2022; Com. 22/7026